Lithospheric buoyancy forces in Africa from a thin sheet approach

D. S. Stamps · L. M. Flesch · E. Calais

Abstract Many features in rift zones and passive margins have been successfully explained by lithospheric stretching models driven solely by tectonic forces. However, the origin of these forces and whether they are sufficient for amagmatic rifting of an initially thick lithosphere remain open questions. We use a thin sheet approach and the CRUST 2.0 model to compute vertically averaged deviatoric stresses arising from horizontal gradients of gravitational potential energy. Computed deviatoric stress directions agree well with earthquake focal mechanisms and stress indicators from the World Stress Map project. We compare the resulting force per unit length with the integrated strength of the lithosphere in the East African Rift and show that buoyancy forces may account for a significant part of the force budget causing continental rifting but are likely insufficient to rupture an initially thick and cold continental lithosphere. This suggests other processes contribute at a significant level to the force balance driving continental rifting in East Africa.

Keywords Continental rifting · East African rift · Deviatoric stresses · Gravitational potential energy

Introduction

Rifting is a fundamental tectonic process that controls the break-up of continents, the development of passive margins, and the initation of ocean basins. Rifting provides the conditions needed to produce oil and geothermal resources and is often associated with volcanic and seismic hazards. Many features in rift zones and passive margins have been successfully explained by lithospheric stretching models (e.g., McKenzie 1978; Wernicke 1981; Lister et al. 1986; Whitmarsh et al. 2001), which assume that lithospheric thinning and crustal extension are driven by far-field stresses from plate motions. However, a number of observations in the East African Rift (EAR), the divergent boundary between the Nubian and Somalian plates (Fig. 1), are difficult to explain with stretching models. For instance, geodetic results in the Main Ethiopian Rift show (1) localized deformation in the rift valley coincident with volcanic systems and (2) lack of border fault activity early on in the rifting process (Bilham et al. 1999). Also, the recent discovery of a diking event in the youthful and poorly extended Natron rift (Tanzania, Fig. 1) shows that magma intrusions can accommodate large amounts of strain during the initial stages of continental rifting and prior to significant crustal thinning (Kendall et al. 2005; Calais et al. 2008). The forces and physical processes at play during continental rifting, therefore, remain to be understood and quantified.

Because the Nubian and Somalian plates are predominantly surrounded by mid-ocean ridges, tractions along their side boundaries contribute little to the deviatoric stress field in the African continent. Deviatoric stresses in Africa should then be dominated by lateral gradients of gravitational potential energy (GPE) in the lithosphere (Coblentz and Sandiford 1994) and/or traction from mantle flow at the base of the lithosphere (e.g., Stoddard and Abbott 1996; Bird 1998a). A number of studies have shown that deviatoric stresses associated with lateral gradients of GPE can significantly contribute to the force balance driving continental deformation and affect the magnitude and style of lithospheric strain (e.g., Molnar and

D. S. Stamps (✉) · L. M. Flesch · E. Calais
Purdue University, 550 Stadium Mall Drive,
West Lafayette, IN 47907, USA
e-mail: dstamps@purdue.edu
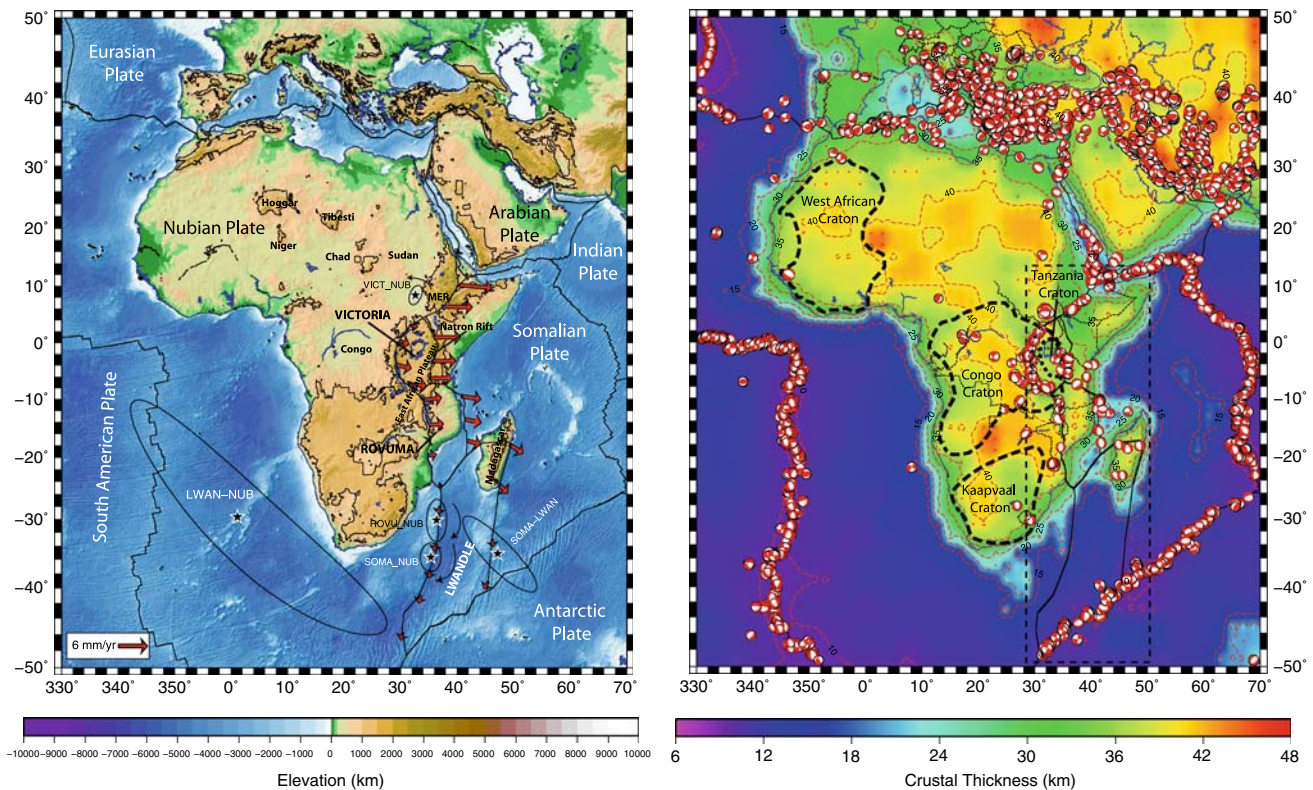
Fig. 1 *Left* ETOPO5 topography with 1000 m contour in Africa and southern Arabia, bathymetry, major plate boundaries, predicted velocities across East African rift plate boundaries (Stamps et al. 2008) (*arrows* show relative velocity of the plate to the east of the boundary with respect to the plate to the west of the boundary), and geographic locations mentioned in the text. *Stars* show Euler poles for plate pairs with their error ellipses (Stamps et al. 2008), with the fixed plate listed second. *VICT* Victoria, *ROV* Rovuma, *LWAN* Lwandle, *NUB* Nubia, *SOMA* Somalia. *Right* Crustal thickness from CRUST 2.0, major craton boundaries from Ritsema and van Heijst (2000) as *thick dashed black lines*, focal mechanisms (CMT catalog) and a *dashed box* outlining the East African Rift

Lyon-Caen 1988; England and Molnar 1997; Flesch et al. 2001; Vergnolle et al. 2007). Here, we use a crustal density model derived from seismic data (CRUST 2.0, Bassin et al. 2000) to compute deviatoric stresses due to lateral gradients of GPE (referred to here as "deviatoric stresses") for Africa and its surroundings. We discuss the pattern and magnitude of these deviatoric stresses and compare them with the strength of the continental lithosphere in East Africa. We show that deviatoric stresses may account for a significant part of the force budget but are not sufficient to rupture an initially thick and cold continental lithosphere.

Tectonic setting

The African continent is characterized by broad high-elevation plateaus in southern and eastern Africa (Fig. 1) which, contrary to other continents such as Asia or South America, are not related to recent compressional tectonics. These plateaus, and their offshore extension in the southeastern Atlantic, define the "African Superswell" (Nyblade and Robinson 1994), a broad topographic anomaly 500 m

higher on average than the global mean. This anomalous topography coincides with a low shear wave velocity province in the deep mantle, the "African Superplume", originating at the core-mantle boundary beneath southern Africa and rising in a NNE-ward direction (Nyblade et al. 2000). The analysis of long-wavelength gravity and topographic relief over Africa shows that more than half of the African Superswell uplift is dynamically supported by convective mantle upwelling associated with the African Superplume (Lithgow-Bertelloni and Silver 1998; Gurnis et al. 2000; Nyblade et al. 2000; Forte and Mitrovica 2001). Other shallower, low-velocity anomalies have been seismically imaged in the upper mantle below eastern Africa (e.g., Nyblade et al. 2000; Weeraratne et al. 2003; Bastow et al. 2005), but their depth extent and connection to the superplume are unclear. Whether or not the African Superplume is solely responsible for the anomalously high topography in Africa, in particular at regional wavelength, remains debated (Burke and Gunnell 2008).

The East African Rift (EAR), the active divergent boundary between the Nubian and Somalian plates, is a 5,000 km long series of fault-bounded depressions that

straddles East Africa in an approximate N-S direction, cutting across the 1,300 km wide, 1,100 m high East African Plateau (Fig. 1). Seismicity in the EAR is moderate, with a few events slightly larger than M7 and mostly extensional focal mechanisms. Albaric et al. (2008) show that earthquake hypocenters in the EAR deepen from north to south along the Eastern rift from 10 to 20 km, whereas they are usually deeper along the Western rift and the Malawi rift (up to 35 km). They argue that this depth distribution is consistent with tectonic provinces (contrasted thermal gradients and basement types) and implies a highly resistant, mafic lower crust.

Recent analyses of geodetic data and earthquake slip vectors in East Africa (Calais et al. 2006; Stamps et al. 2008) show that (1) present-day Nubia-Somalia motion is consistent with the ~3 Myear average, (2) the kinematics of the plate boundary zone is best described with a model that includes three minor sub-plates defined using the distribution of seismicity (Victoria, Rovuma, and Lwandle), and (3) extension is directed ~E-W all along the rift, with rates decreasing from 6–7 mm/year in the Main Ethiopian Rift, 3–4 mm/year in the central EAR, to <1 mm/year south of Mozambique. GPS velocities at the 14 best-determined geodetic sites on the Nubia plate are consistent with a single rigid rotation with an average residual of ~2mm/year (95% confidence level), close to the precision level of GPS velocity estimates (Nocquet et al. 2006; Stamps et al. 2008). This shows that the Nubia plate behaves rigidly at the current precision level of the GPS measurements.

Crustal structure in Africa is not well known, except for specific regions where temporary seismic networks were deployed (e.g., Bastow et al. 2005; Birt et al. 1997; Ibs-von Seht et al. 2001). Most of these studies were included in CRUST 2.0, a global crustal model at a 2 × 2° resolution (Bassin et al. 2000) with seven vertical layers (ice, water, soft sediments, hard sediments, upper crust, middle crust, lower crust). CRUST 2.0 will be our basis for computing GPE and the horizontal deviatoric stresses resulting from its lateral gradients. Because it is interpolated from actual seismic data, CRUST 2.0 provides a reasonably accurate description of crustal structures over broad areas, although it may not be able to resolve small-scale features. Local inaccuracies will impact the calculations of GPE gradients but will not affect our conclusions since we are interested in length scales greater than the 2 × 2° spatial resolution of CRUST 2.0. Detailed studies will need to utilize a more accurate crustal structure model of Africa. Figure 1 shows that crustal thicknesses on the African continent range from about 30 km at the coastlines to up to close to 50 km in western Mali and southeastern Angola and are not directly correlated with topography. In particular, the high topography surrounding the EAR corresponds to crustal

thicknesses between 30 and 35 km, less than the average for the continent.

Deviatoric stresses associated with lateral gradients in GPE

Method

We compute vertically averaged deviatoric stresses resulting from lateral gradients in GPE by treating the lithosphere as an incompressible, viscous continuum where the 3-D force balance can be written as:

$$\frac{\partial \sigma_{ij}}{\partial x_j} + \rho g z_i = 0 \tag{1}$$

(e.g. Houseman and England 1986), where g is the gravitational acceleration, ρ is density, z is the vertical direction. σ_{ij} is the total stress tensor defined by:

$$\sigma_{ij} = \tau_{ij} + \frac{\sigma_{kk}}{3}\delta_{ij} = \tau_{ij} + (\sigma_{zz} - \tau_{zz})\delta_{ij} \tag{2}$$

Here, τ_{ij} is the deviatoric stress tensor, σ_{kk} is the trace of the total stress tensor, and δ_{ij} is the Kronecker delta. Substituting Eq. (2) into Eq. (1) and assuming that gradients of shear tractions on vertical planes are negligible, we apply the thin sheet approximation (e.g. Bird and Piper 1980; England and McKenzie 1982) and vertically average deviatoric stresses over the thickness of the lithosphere, which yields the following force balance equations:

$$-\frac{\partial \overline{\sigma}_{zz}}{\partial x} = 2\frac{\partial \overline{\tau}_{xx}}{\partial x} + \frac{\partial \overline{\tau}_{yy}}{\partial x} + \frac{\partial \overline{\tau}_{xy}}{\partial y} \tag{3}$$

$$-\frac{\partial \overline{\sigma}_{zz}}{\partial y} = 2\frac{\partial \overline{\tau}_{yy}}{\partial y} + \frac{\partial \overline{\tau}_{xx}}{\partial y} + \frac{\partial \overline{\tau}_{xy}}{\partial x} \tag{4}$$

(Flesch et al. 2001) where $\overline{\sigma}_{zz}$ is the vertically averaged vertical stress for a lithospheric column and $\overline{\tau}_{\alpha\beta}$ are vertically averaged deviatoric stresses.

The vertically integrated vertical stress is defined as:

$$\overline{\sigma}_{zz} = -\frac{1}{\overline{h}}\int\limits_0^h \left(\int\limits_0^z \rho(z')g dz'\right)dz \tag{5}$$

where $\overline{h}$ is the average lithospheric thickness, $\rho(z')$ is the depth-dependent density, z is depth, and g is the gravitational acceleration. $\overline{\sigma}_{zz}$ is expressed in units of potential energy per unit volume (Flesch et al. 2001). Depth-dependent density within the crust is computed using CRUST 2.0.

Equations (3) and (4) are underdetermined (with three unknowns $\overline{\tau}_{xx}, \overline{\tau}_{yy}, \overline{\tau}_{xy}$) but can be solved either by assuming an a priori rheology (e.g. Bird and Piper 1980; England

and McKenzie 1982) or by assuming that the solution possesses the minimum surface integral of the second invariant of deviatoric stress (Flesch et al. 2001). This latter strategy, which does not require a priori assumptions on the lithospheric rheology, is the one used here. We used an average lithospheric thickness of 100 km, a widely used value for lithospheric thickness (Haines and Holt 1993; Flesch et al. 2001; Ghosh et al. 2008). Equations (3) and (4) can then be solved for vertically averaged deviatoric stresses associated with gradients of gravitational potential energy using standard finite element methods. This approach neglects tractions at the base of the lithosphere, which may contribute additional stresses (e.g., Bott 1992; Bird et al. 2008) and need to be addressed by further research.

Results

Since the magnitude of GPE, and correspondingly the magnitudes of vertically averaged deviatoric stresses derived from gradients in GPE (see Fig. 6 for an example vertical distribution of stresses), depends on the density structure of each lithospheric column from the surface down to a given depth $\bar{h}$, it is affected by mantle density variations. We therefore compare two models, one with a uniform mantle density of 3,300kg/m^3, the other with a laterally variable density (Fig. 2). In the first case, we find significant deviations from isostatic equilibrium over the African continent. The difference between actual and predicted topography (Fig. 3, left) is negative overall in Africa, except in the Ethiopian plateau-Red Sea area and along the Eastern and Western rifts. For the second case, we estimate the mantle density required to keep each lithospheric column in isostatic balance with respect to a reference mid-ocean ridge of density 3,196km/m^3. The difference between the 3,300kg/m^3 average mantle density and the estimated one ($\Delta\rho$), shown on Fig. 3 (right), mimics the dynamic topography patterns, as expected. Areas of positive $\Delta\rho$ in the Ethiopian plateau-Red Sea area and along the Eastern and Western rifts indicate that topography in these areas is maintained by negative (i.e., buoyant) gravity anomalies in the upper mantle. This is consistent with seismic tomography studies that report seismic velocity anomalies in the upper mantle are indicative of positive thermal anomalies (e.g., Green et al. 1991; Nyblade et al. 2000; Davis and Slack 2002; Bastow et al. 2005).
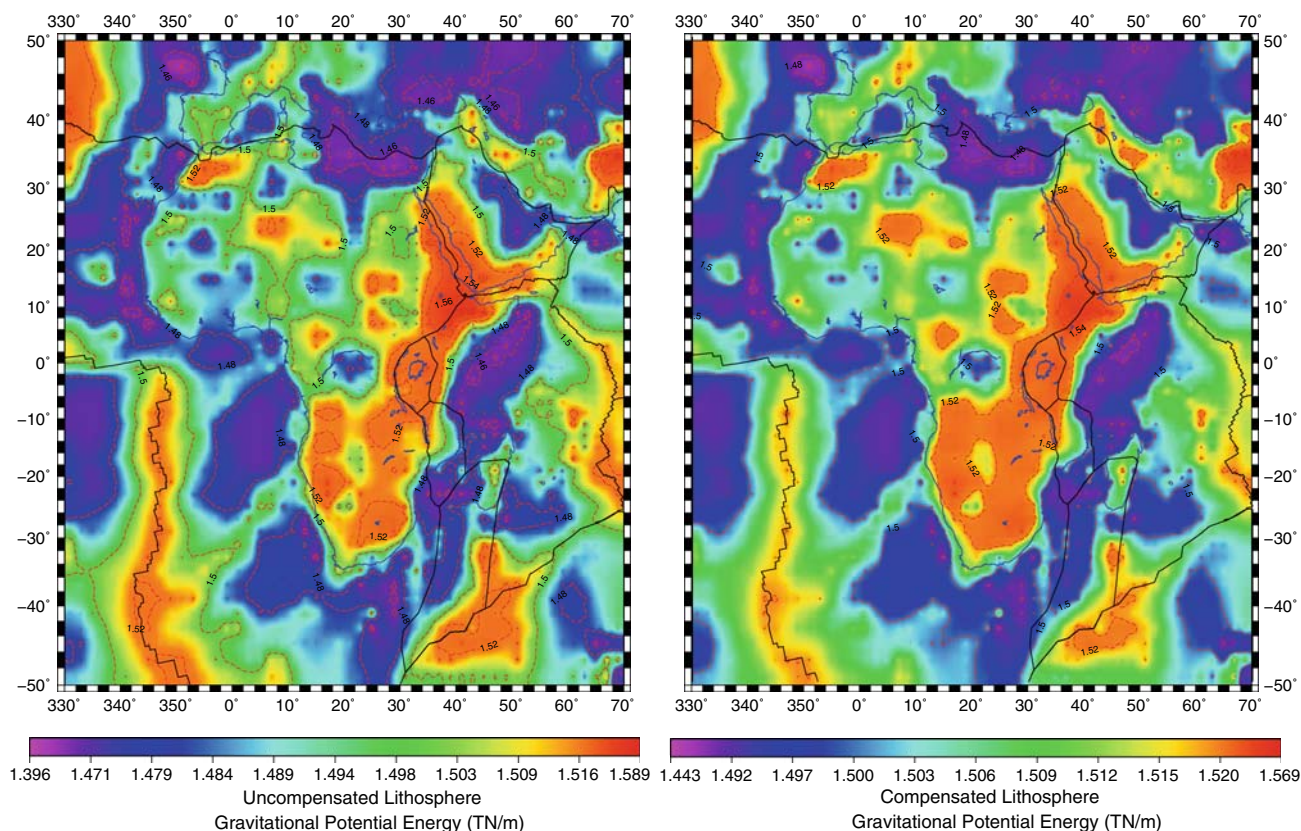
Fig. 2 Magnitudes of gravitational potential energy (vertically integrated vertical stress). Contour interval is 0.02 TN/m. *Left* Uncompensated model with uniform mantle density (3,300 kg/m^3). *Right* Compensated model (compensation depth = 100 km) with the laterally variable mantle density shown in Fig. 3 *right*
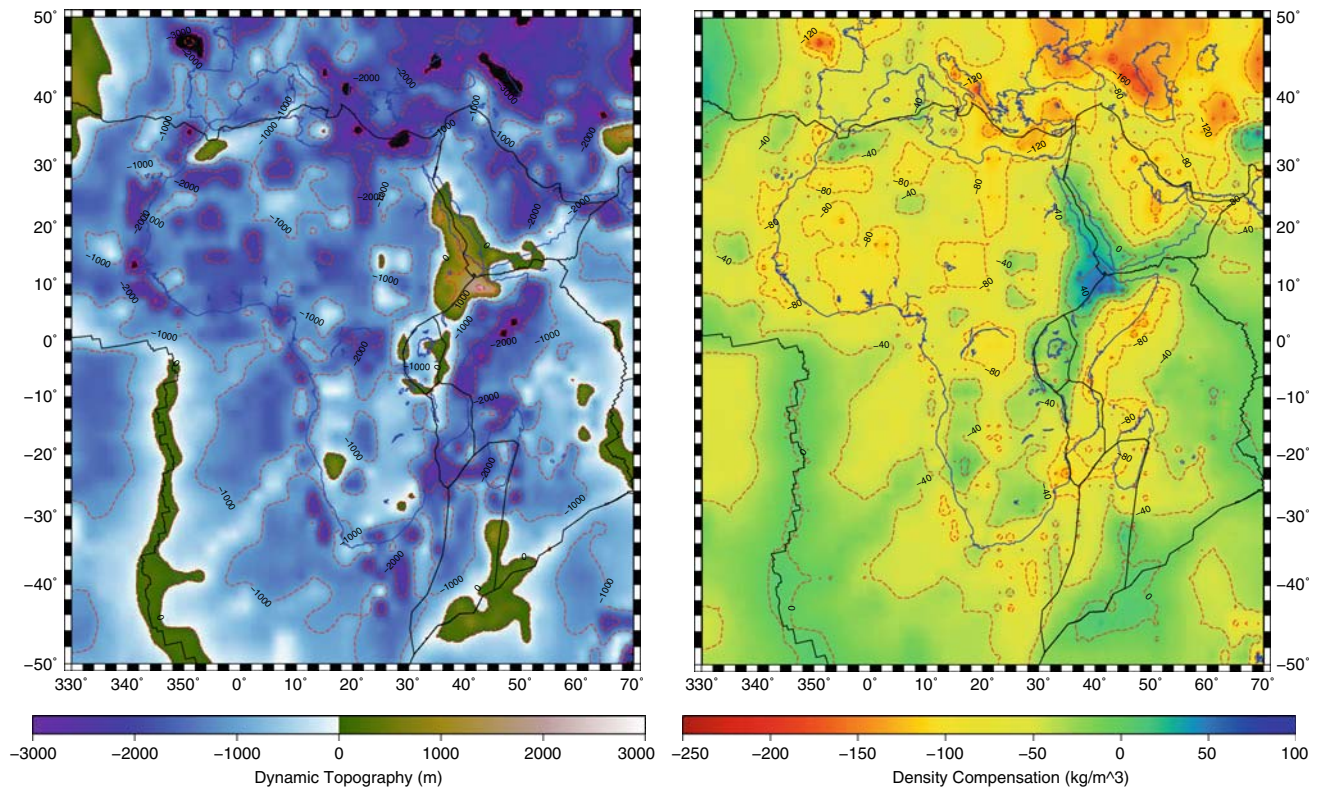
Fig. 3 *Left* Predicted dynamic topography using a constant mantle density of 3,300kg/m³. *Right* Estimated mantle density ($\Delta\rho$) required for the isostatic balance of the lithosphere for a 100 km compensation depth with respect to a standard mid-oceanic ridge column of density 3,186 kg/m³

Actual topography combines an isostatic component (determined by the crustal and lithospheric mantle density structure) and a dynamic component (resulting from radial mantle tractions). In the following, we discuss both models (uncompensated and compensated) but favor the compensated one because it accounts for both the lateral variations in mantle density and radial mantle tractions.

Figure 4 shows that patterns of tensional (red) and compressional (black) deviatoric stresses in continental Africa correlate well with topography for both compensated and uncompensated cases. Deviatoric stresses are tensional in areas with higher elevations (e.g., southern and eastern Africa, Hoggar-Tibesti, central Madagascar), close to neutral in low-elevation areas, and compressional in low-elevation sedimentary basins (e.g., Congo, Niger, and Chad basins). Outside of continental Africa, tensional ridge-parallel deviatoric stresses along oceanic spreading centers reflect their higher gravitational potential due to ridge elevation with respect to the surrounding. Compressional deviatoric stresses in ocean basins and passive margins reach 10 MPa and tend to increase from the ridges toward the older (hence denser and thicker) parts of the basins with similar patterns in ancient oceanic basins (Mediterranean, Black Sea).

Deviatoric stresses are larger overall for the uncompensated case (26.9 MPa maximum in EAR), but the patterns of tension and compression are the same as the compensated case (18.9 MPa maximum in EAR; Fig. 4). The difference in deviatoric stress magnitudes results from the fact that the mantle density required to compensate CRUST 2.0 is overall greater than the 3,300km/m³ mantle average (positive $\Delta\rho$ on Fig. 3). This results in decreasing the magnitude of the lateral gradients in GPE and, consequently, in decreasing the magnitude of associated deviatoric stresses.

Discussion

Deviatoric stresses and stress/strain indicators

Coblentz and Sandiford (1994) were first to calculate a deviatoric stress field for the African continent and its surroundings. Their method uses a simple lithospheric density model consistent with long-wavelength geoid anomalies. The CRUST 2.0 density model used here is more accurate as it is based on seismic surveys, but principal deviatoric stress direction and deviatoric stress
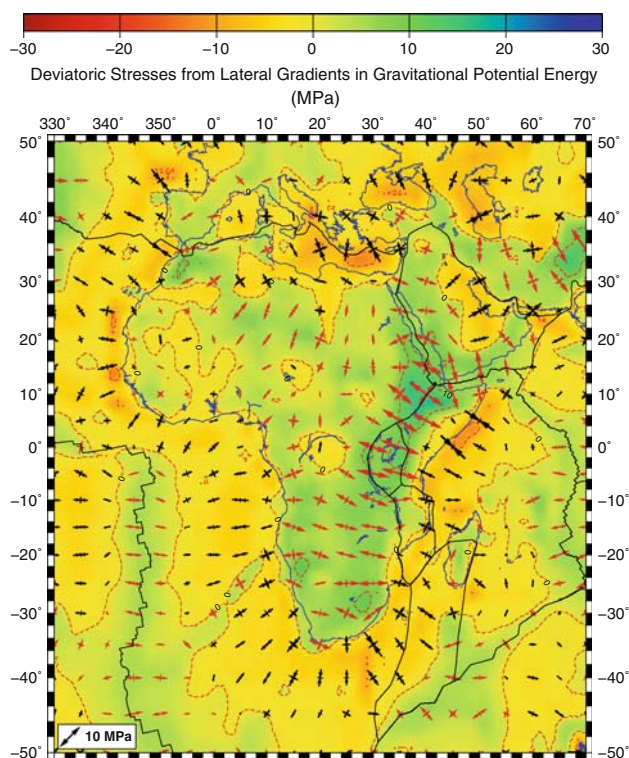
Fig. 4 Vertically averaged deviatoric stresses associated with lateral gradients in gravitational potential energy for a 100-km thick, compensated, lithosphere. *Color background* shows the second invariant (magnitude) of the stress tensor. *Arrows* show the direction and magnitude of the principal horizontal stresses. *Red* tensors represent principally extensional stresses and *black* tensors show compressional stresses. Contour interval in *red dashed line* is 10 MPa. This model is compensated by laterally varying sub-crustal mantle densities of each lithospheric column to 100 km so that it is in isostatic balance with a standard mid-oceanic ridge column of density 3,186 kg/m³

Fig. 5 Comparison between SH_max directions from the World Stress Map (*WSM*) project and from our model. All A-, B-quality WSM indicators in this region are categorized "normal". C- and D-quality stress indicators may not be reliable indicators of regional-scale SH_max (Zoback 1992) and are therefore not used here. Seismicity ($M > 5$) from the USGS-NEIC database (1973–present) is shown with *black dots*. *Black lines* show approxiamte location of active faults in the East Africa rift

magnitudes agree well with Coblentz and Sandiford's results. In particular, both models find similar stress magnitudes in the EAR, from 15 MPa around the Ethiopian plateau to 9 MPa in the central rift (Tanzania), and in southern Africa (around 8 MPa). Our CRUST 2.0-based model, however, provides a higher spatial resolution deviatoric stress field. For example, although the deviatoric stress field in Africa is generally tensional, our model shows that compressional deviatoric stresses centered on the Congo basin are consistent with compressional focal mechanisms in central Congo (Fig. 1 right and Fig. 5).

The style and directions of deviatoric stresses in Africa and surroundings are consistent overall with focal mechanisms (Fig. 1) and maximum horizontal compressive deviatoric stress directions (SH_max) for A- and B-quality indicators from the World Stress Map (WSM; Zoback 1992; Heidbach et al. 2008; Fig. 5). We did not use C- and D-quality indicators since they may not be reliable indicators of regional-scale SHmax, as discussed in Zoback

(1992). The African continent is overall under tensional deviatoric stresses, reaching up to 15 MPa in the northernmost part of the EAR. Higher tensional deviatoric stresses correlate with the trace of the EAR, with deviatoric stress magnitudes decreasing southward to about 5 MPa at the southern termination of the Malawi rift. Deviatoric stress directions agree well with earthquake focal mechanisms and WSM stress indicators, consistent with E-W to ESE-WNW tension along the Main Ethiopian Rift and further south along the Western Rift, Eastern Rift, and the Malawi Rift.

Deviatoric stress magnitudes are high outside of the EAR as well, in particular in the southern part of the continent, and may explain the off-rift seismicity observed throughout Africa. Principal deviatoric stress directions are consistent with earthquake focal mechanisms in South Africa, southeastern Congo (Mweru rift), and Zambia (Kariba graben).

Principal tensional deviatoric stresses along the active Mweru rift, Kariba graben, and Okawango faults are oriented NW-SE, perpendicular to these structures, which could explain normal faulting and incipient rifting in these regions. Our calculations also predict compressional deviatoric stresses consistent with observations of reverse focal mechanisms along Africa's passive margins offshore

Mauritania and in the Gulf of Guinea (Fig. 1). The same holds for the compressional focal mechanisms observed in central Congo, consistent with the computed compressional deviatoric stresses.

The accuracy of deviatoric stresses computed here is limited by the accuracy of the CRUST 2.0 model. In comparison with its predecessor CRUST 5.1, CRUST 2.0 uses more seismic data, benefits from a $1 \times 1°$ digital map of sediment thicknesses, and integrates updated ice thicknesses (accurate within 250m). However, CRUST 2.0 still suffers from limited data in many areas, particularly in Africa where access to the field is restricted for geophysical experiments. To mitigate this issue, CRUST 2.0 uses 360 type-profiles based on seismic studies and statistical averages of regions with similar crustal structures (e.g. oceanic plateaus, Proterozoic cratons, island arcs) to be used in areas with little or no seismic information like northern, western, central, and parts of eastern Africa. This makes our model susceptible to the definitions of geologic provinces in regions without seismic information. Fortunately, crustal structure across the Tanzania Craton, in the Eastern Branch, the Main Ethiopian Rift, and the region centered on the Afar plume are constrained by seismic studies rather than type-profiles alone (e.g. Simiyu and Keller 1997; Berckhemer et al. 1975; Birt et al. 1997; Prodehl and Mechie 1991). Pasyanos and Nyblade (2007) compared CRUST 2.0 with a new seismically based crustal structure model. In East Africa, they report crustal thinning in southern Sudan and northern Kenya that is not accounted for in CRUST 2.0. The largest difference is in Madagascar, where seismic data indicate a 25–35 km thick crust (deWit 2003) versus 40 km in CRUST 2.0. These differences are however small and local and will therefore not significantly affect the overall magnitude or pattern of deviatoric stresses in Africa, which is dominated by the effects of long-wavelength topography and crustal thickness variations.

Strength of the lithosphere

The magnitude of the deviatoric stresses derived from lateral gradients in GPE found throughout the East African Rift, on the order of 10 MPa, corresponds to a cumulative force of 1.5 TN/m for a 150 km lithosphere and 1.0 TN/m for a 100-km-thick lithosphere. Whether this force is sufficient to initiate and sustain continental rupture is a debated issue. In most traditional models of rifting (e.g., Wernicke 1981; Lister et al. 1986), continental rupture occurs solely as a result of tectonic forces. However, it has been pointed out that the tectonic force required to initiate and maintain break-up of initially thick continental lithosphere may be up to an order of magnitude larger than available (e.g., Kusznir and Park 1987; Hopper and Buck 1993).
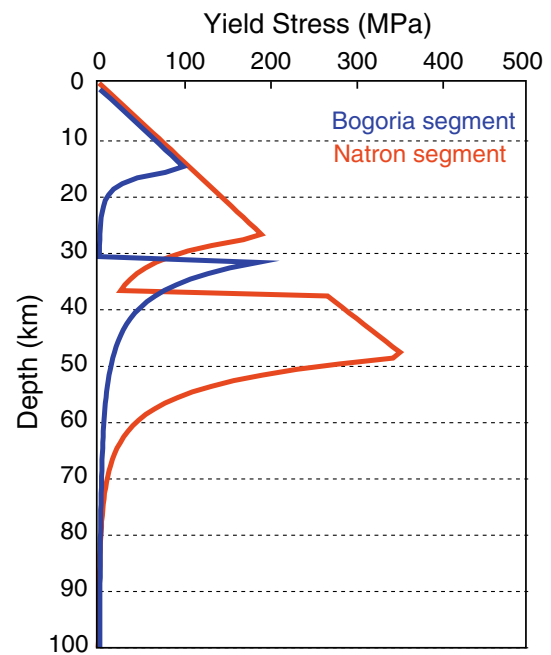
Fig. 6 Yield stress envelopes for the weaker Bogoria segment of the Eastern rift and for the stronger Balangida segment (see Fig. 5 for locations). Flow law parameters are from Albaric et al. (2008), heat flow from Nyblade et al. (1990), strain rate from Stamps et al. (2008)

We computed the vertically integrated strength of the lithosphere in the EAR based on recent results from Albaric et al. (2008), who used seismicity depth distribution in the central part of the EAR to quantify lithospheric rheology. Albaric et al. (2008) found significant regional variations of the thermo-mechanical properties of the lithosphere along the EAR with an increase in lithospheric strength from north to south along the Eastern Rift. Figure 6 shows the yield stress envelope for the one of the weakest (Bogoria) and strongest (Balangida) segments of the Eastern Rift, using the parameters listed by Albaric et al. (2008) for the crust and assuming wet olivine for the lithospheric mantle. Heat flow values are taken from Nyblade et al. (1990; 104 mW/m^2 for Bogoria and 46 mW/m^2 for Natron) and a strain rate of $5 \times 10^{-15} s^{-1}$ (purely extensional) is assumed, following the kinematic model of Stamps et al. (2008). Under these assumptions, we find that the vertically integrated strength of the lithosphere varies from 4 TN/m (Bogoria) to 9 TN/m (Natron), consistent with previously reported values for the extensional strength of the lithosphere at low strain rates (~ 4 TN/m, Houseman and England 1986). The comparison between the cumulative force per unit length available from GPE and the strength of the lithosphere in the EAR therefore shows that buoyancy forces may account for a significant part of the force budget causing continental rifting (Coblentz and Sandiford 1994), but are likely insufficient to rupture an initially thick and cold continental lithosphere.

Conclusions

This new analysis of deviatoric stresses arising from lateral gradients in GPE in the African lithosphere based on the CRUST 2.0 crustal model shows a good agreement with independent stress and strain observations in Africa. These deviatoric stresses result largely from the high elevations of southern and eastern Africa, a feature that possibly results from mantle flow associated with the African Superplume (Conrad and Gurnis 2003).

Once quantified, it appears that deviatoric stresses alone are not sufficient to overcome the strength of the continental lithosphere in the Eastern rift. A similar conclusion likely holds for large segments of the EAR since the Bogoria area, where yield stress is still ~ 3 times larger than available deviatoric stresses, has one of the highest heat flow values within the EAR. These results therefore support—and further quantify—the so-called "stress paradox" of continental rifts (Buck 2004), where tectonic forces alone are not sufficient for amagmatic rifting of an initially thick lithosphere.

The discrepancy between lithospheric strength and deviatoric stresses indicates that other processes contribute significantly to the force balance driving continental rifting in East Africa. For instance, Buck (2004) showed that dike intrusions reduce the force required to cause extensional yielding of continental lithosphere by a factor of up to six, thanks to the positive buoyancy of melt and the reduction in plate strength by magmatic heating. This magma-assisted rifting model finds support in the recent dike intrusion captured in the Natron basin (Calais et al. 2008), an event that shows features similar to other earthquake swarms in the Eastern rift.

Alternatively, mantle tractions—not explicitly considered in this analysis—may significantly contribute to driving lithospheric extension in Africa. For instance, Quéré and Forte's (2006) mantle flow model predicts that the EAR opens solely in response to large-scale mantle flow without requiring upwelling plumes directly beneath the rift. Further steps in this analysis require quantifying the contribution of magmatic processes and mantle tractions to driving and sustaining forces contributing to continental rifting.

References

Albaric J, Déverchére J, Petit C, Perrot J, Le Gall B (2008) Crustal rheology and depth distribution of earthquakes: insights from the central and southern East African rift system. Tectonophysics doi:10.1016/j.tecto.2008.05.021

Bassin C, Laske G, Masters G (2000) The current limits of resolution for surface wave tomography in North America. EOS Trans AGU 81:F897. Available at http://mahi.ucsd.edu/Gabi/rem.html

Bastow ID, Stuart GW, Kendall J-M, Ebinger CJ (2005) Upper-mantle seismic structure in a region of incipient continental break-up: northern Ethiopian rift. Geophys Res Lett 162:479–493

Berckhemer H, Baier B, Bartelson H, Behle A, Burkhardt H, Gebrande H, Makis J, Menzel H, Miller H, Vees R (1975) Deep seismic soundings in the Afar region and on the highland of Ethiopia. In: Pilger A, Rósler R (eds) Afar between continental and oceanic rifting. pp 89–107

Bilham R, Bendick R, Larson K, Mohr P, Braun J, Tesfaye S, Asfaw L (1999) Secular and tidal strain across the main Ethiopian rift. Geophys Res Lett 26(18):2789–2792

Bird P (1998) Testing hypotheses on plate-driving mechanisms with global lithosphere models including topography, thermal structure, and faults. J Geophys Res 103(B5):10115–10129

Bird P, Liu Z, Rucker WK (2008) Stresses that drive the plates from below: definitions, computational path, model optimization, and error analysis. J Geophys Res 113(B11406) doi:10.1029/2007JB005460

Bird P, Piper K (1980) Plane-stress finite-element models of tectonic flow in southern California. Phys Earth Planet Inter 21(2–3):158–175

Birt CS, Maguire PKH, Khan MA, Thybo H, Keller GR, Patel J (1997) The influence of pre-existing structures on the evolution of the southern Kenya Rift Valley—evidence from seismic and gravity studies. Tectonophysics 278(1–4):211–242

Bott MHP (1992) Modelling the loading stresses associated with active continental rift systems. Tectonophysics 215:99–115

Buck RW (2004) Consequences of asthenospheric variability on continental rifting. In: Karner GD, Taylor B, Driscoll NW, Kohlstedt DL (eds) Special volume on rupturing continental lithosphere of the margins program. pp 1–59

Buck WR, Lavier LL, Poliakov ANB (1999) How to make a rift wide. Phil Trans Res Soc London A 357:671–693

Burke K, Gunnell Y (2008) The African erosion surface: a continental-scale synthesis of geomorphology, tectonics, and environmental change over the past 180 million years. Geol Soc Am Memoir 201

Calais E, d'Oreye D, Albaric J, Deschamps A, Delvaux D, Dverchére J, Ebinger CJ, Ferdinand RW, Kervyn F, Macheyeki AS, Oyen A, Perrot J, Saria E, Smets B, Stamps DS, Wauthier C (2008) Strain accommodation by slow slip and dyking in a youthful continental rift, East Africa. Nature 456:783–787 doi:10.1038/nature07478

Calais E, Ebinger CJ, Hartnady C, Nocquet J-M (2006) Kinematics of the East African rift from GPS and earthquake slip vector data. In: Yirgu G, Ebinger CJ, Maguire PKH (eds) The Afar volcanic province within the East African rift system. Geol Soc Spec Pub, vol 259, pp 9–22

Coblentz DD, Richardson RM, Sandiford M (1994) On the gravitational potential of the Earth's lithosphere. Tectonics 13:929–945

Coblentz DD, Sandiford M (1994) Tectonic stresses in the African plate: constraints on the ambient lithospheric stress state. Geology 22:831–834

Conrad CP, Gurnis M (2003) Seismic tomography, surface uplift, and the breakup of Gondwanaland: integrating mantle convection backwards in time. Geochem Geophys Geosyst 4(3) doi:10.1029/2001GC000299

Davis P, Slack PD (2002) The uppermost mantle beneath the Kenya dome and relation to melting, rifting and uplift in East Africa. Geophys Res Lett 29(7) doi:10.1029/2001GL013676

deWit M (2003) Madagascar: heads it's an island tails it's a continent. Annu Rev Earth Planet Sci (31):213–148 doi:10.1146/annurev.earth.31.100901.141337

England P, McKenzie DP (1982) A thin viscous sheet model for continental deformation. Geophys J R Astron Soc 70:395–321

England P, Molnar P (1997) Active deformation of Asia: from kinematics to dynamics. Science 278(5338):647–650 doi:10.1126/science.278.5338.647

Flesch LM, Haines JA, Holt WE (2001) Dynamics of the India-Eurasia collision zone. J Geophys Res 106:16435–16460

Forte AM, Mitrovica JX (2001) Deep-mantle high-viscosity flow and thermochemical structure inferred from seismic and geodynamic data. Nature 410(6832):1049–1056

Forte AM, Mitrovica JX, Moucha R, Simmons NA, Grand SP (2007) Descent of the Farallon slab drives localized mantle flow below New Madrid seismic zone. Geophys Res Lett 34(L04308) doi:10.1029/2006GL027895

Ghosh A, Holt WE, Wen L, Haines AJ, Flesch LM (2008) Joint modeling of lithosphere and mantle dynamics elucidating lithosphere-mantle coupling. Geophys Res Lett 35(L16309) doi:10.1029/2008GL034365

Green WV, Achauer U, Meyer RP (1991) A three-dimensional seismic image of the crust and upper mantle beneath the Kenya rift. Nature 354:199–203 doi:10.1038/354199a0

Gurnis M, Mitrovica JX, Ritsema J, van Heist H-J (2000) Constraining mantle density structure using geological evidence of surface uplift rates: the case of the African Superplume. Geochem Geophys Geosyst 1 doi:1999GC000035

Haines AJ, Holt WE (1993) A procedure for obtaining the complete horizontal motions within zones of distributed deformation from the inversion of strain rate data. J Geophys Res 98(B7):12057–12082

Heidbach O, Tingay M, Barth A, Reinecker J, Kurfeß BD, Müller B (2008) The World Stress Map database release 2008 doi:10.1594/GFZ.WSM.Rel2008

Hopper JR, Buck, WR (1993) The initiation of rifting at constant tectonic force: role of diffusion creep. J Geophys Res 98(B9):16213–16221

Houseman GA, England PC (1986) Finite strain calculations of continental deformation 1. Method and general results for convergent zones. J Geophys Res 91:3651–3663

Ibs-von Seht M, Blumenstein S, Wagner R, Hollnack D, Wohlenberg J (2001) Seismicity, seismotectonics and crustal structure of the southern Kenya Rift—new data from the Lake Magadi area. Geophys J Int 146:469–453

Kendall J-M, Stuwart GW, Ebinger CJ, Bastow ID, Keir D (2005) Magma-assisted rifting in Ethiopia. Nature 433:146–148

Kusznir N, Park R (1987) The extensional strength of the continental lithosphere: its dependence on geothermal gradient, and crustal composition and thickness. In: Coward MP, Dewey JF, Hancock PL (eds) Continental extensional tectonics. Geol Soc Spec Publ vol 28, pp 35–85

Langston, CA, Nyblade, AA, Owens, TJ (2002) Regional wave propagation in Tanzania, East Africa. J Geophys Res 107(B1) doi:10.1029/2001JB000167

Lin J, Parmentier EM (1989) Mechanisms of lithospheric extension at mid-ocean ridges. Geophys J 96:1–22

Lister GS, Etheridge MA, Symonds PA (1986) Detachment faulting and the evolution of passive continental margins. Geology 14:246–250

Lithgow-Bertelloni C, Silver PG (1998) Dynamic topography, plate driving forces, and the African superswell. Nature 395:269–272

McKenzie, D (1978) Some remarks on the development of sedimentary basins. Earth Planet Sci Lett 40:25–32

Molnar P, Lyon-Caen H (1988) Some simple physical aspects of the support, structure, and evolution of mountain belts. Geol Soc Spec Pub 218:179–207

Mooney WD, Laske G, Masters TG, CRUST 5.1: a global crustal model at $5 \times 5°$. J Geophys Res 103(B1):727–747

Nocquet JM, Willis P, Garcia S (2006) Plate kinematics of Nubia-Somalia using a combined DORIS and GPS solution. J Geod 80:591–607

Nyblade AA, Pollack HN, Jones DL, Podmore F, Mushayandebvu M (1990) Terrestrial heat flow in east and southern Africa. J Geophys Res 95(B11):17371–17384

Nyblade AA, Owens TJ, Gurrola H, Ritsema J, Langston CA (2000) Seismic evidence for a deep upper mantle thermal anomaly beneath East Africa. Geology 28(7):599–602

Nyblade AA, Robinson SW (1994) The African Superswell. Geophys Res Lett 21(9):765–768

Pasyanos ME, Nyblade, AA (2007) A top to bottom lithospheric study of Africa and Arabia. Tectonophysics 444:27–44

Prodehl C, Mechie J (1991) Crustal thinning in relationship to the evolution of the Afro-Arabian rift system: a review of seismic refraction data. Tectonophysics 198(2–4):311–327

Ritsema J, Nyblade AA, Owen TJ, Langston CA, VanDecar JC (1998) Upper mantle seismic velocity structure beneath Tanzania, east Africa: implications for the stability of cratonic lithosphere. J Geophys Res 109(B9):21201–21213

Ritsema J, van Heijst H (2000) New seismic model of the upper mantle beneath Africa. Geology 28(1):63–66

Quéré S, Forte AM (2006) Influence of past and present-day plate motions on spherical models of mantle convection: implications for mantle plumes and hotspots. Geophys J Int 165:1041–1057

Simiyu SM, Keller GR (1997) Structure and dynamic processes in the lithosphere of the Afro-Arabian rift system. Tectonophysics 278(1–4):291–313

Stacey FD (1992) Physics of the earth, 3rd edn. Cambridge University Press, New York

Stamps DS, Calais E, Saria E, Hartnady C, Nocquet, J-M, Ebinger CJ, Fernandes RM (2008) A kinematic model for the East African rift. Geophys Res Lett 35(L05304) doi:10.1029/2007GL03278

Stein S, Wysession M (2006) An introduction to seismology, earthquakes, and earth structure. Blackwell, London

Stoddard PR, Abbott DH (1996) The influence of the tectosphere upon plate motion. J Geophys Res 101:5425–5433

Vergnolle M, Calais E, Dong L (2007) Dynamics of continental deformation in Asia. J Geophys Res 112(B11403) doi:10.1029/2006JB004807

Weeraratne DS, Forsyth DW, Fischer KM, Nyblade AA (2003) Evidence for an upper mantle plume beneath the Tanzanian craton from Rayleigh wave tomography. J Geophys Res 108(B9) doi:10.1029/2002JB002273

Wernicke B (1981) Low-angle normal faults in the Basin and Range Province: nappe tectonics in an extending orogen. Nature 291:645–648 doi:10.1038/291645a0

Whitmarsh RB, Manatschal G, Minshull TA (2001) Evolution of magma-poor continental margins from rifting to seafloor spreading. Nature 413:150–154

Zoback ML (1992) First- and second-order patterns of stress in the lithosphere: the world stress map project. J Geophys Res 97(B8):11703–11728